



## OPEN

## Neural Mechanism for Sensing Fast Motion in Dim Light

Ran Li<sup>1,2</sup> & Yi Wang<sup>1</sup><sup>1</sup>State Key Laboratory of Brain and Cognitive Science, Institute of Biophysics, Chinese Academy of Sciences, Beijing 100101, China, <sup>2</sup>University of Chinese Academy of Sciences, Beijing 100049, China.SUBJECT AREAS:  
ANIMAL PHYSIOLOGY  
NEUROPHYSIOLOGY  
MOTION  
STRIATE CORTEXReceived  
22 March 2013Accepted  
22 October 2013Published  
7 November 2013Correspondence and  
requests for materials  
should be addressed to  
Y.W. (yiwang@ibp.  
ac.cn)

Luminance is a fundamental property of visual scenes. A population of neurons in primary visual cortex (V1) is sensitive to uniform luminance. In natural vision, however, the retinal image often changes rapidly. Consequently the luminance signals visual cells receive are transiently varying. How V1 neurons respond to such luminance changes is unknown. By applying large static uniform stimuli or grating stimuli altering at 25 Hz that resemble the rapid luminance changes in the environment, we show that approximately 40% V1 cells responded to rapid luminance changes of uniform stimuli. Most of them strongly preferred luminance decrements. Importantly, when tested with drifting gratings, the preferred speeds of these cells were significantly higher than cells responsive to static grating stimuli but not to uniform stimuli. This responsiveness can be accounted for by the preferences for low spatial frequencies and high temporal frequencies. These luminance-sensitive cells subserve the detection of fast motion under the conditions of dim illumination.

Our ability to interpret responses of neurons in the primary visual cortex (V1) to movies of natural scenes is limited<sup>1–3</sup>. The neuronal responses to the attributes of images play crucial roles in constructing the representation of daily vivid scenes from retinal images<sup>4,5</sup>. The classic studies in this field are predominantly focused on contrast without reporting the coding of uniform luminance<sup>6–16</sup>. This has led to a poor understanding of the responses of V1 cells to uniform luminance in comparison with what is known of their responses to contrast.

The roles of the uniform luminance-sensitive cells in visual functions remain largely unclear<sup>17–21</sup>. Early studies showed that V1 cells respond to diffuse illumination with sustained, transient, or slowly adapting discharges<sup>22–24</sup>. V1 cells also respond to the luminance of large patches of static uniform stimuli<sup>19,25</sup>. V1 responses have been shown to represent the brightness of uniform surfaces<sup>17,19,26,27</sup>. Moreover, V1 cells respond to uniform luminance modulated sinusoidally in time<sup>20,21</sup>. The response magnitudes of V1 cells depend on the levels of the stimulus luminance<sup>19,22,25</sup>. Response profiles of most V1 cells to large uniform stimuli show a monotonic increase or decrease as a function of luminance, but a minority show a V-shaped profile. The V profiles are often time-dependent with monotonic responses more evident in the later period of the stimulation<sup>19</sup>. Some cells respond maximally to the intermediate luminances when the stimulus luminance is slowly modulated sinusoidally<sup>20,21</sup>.

A few studies<sup>18,21,25</sup> have directly compared responses of V1 cells to uniform luminance and contrast stimuli. To large uniform spots with various luminances brighter than the background, orientation selective cells show saturated responses to luminances over a limited range, while cells without orientation selectivity respond differentially to luminance over a larger range<sup>25</sup>. When stimulus size increases, responses to uniform luminance either increase or decrease; the effects do not reliably correlate with those to contrast gratings<sup>18</sup>. In response to a large patch of stimulation, V1 cells form two main groups: luminance-contrast cells that respond to both uniform luminance and contrast and contrast cells that respond only to contrast but not to uniform luminance. Responses to uniform luminance are weak in comparison with those to contrast<sup>21</sup>. Luminance-contrast cells tend to have large receptive fields (RFs), low spatial frequencies, and weaker orientation selectivity than contrast cells. The responses of contrast cells to contrast signals are linearly correlated to the spatial ON-OFF structure of the RF, but those of luminance-contrast cells to contrast are not<sup>21</sup>. Other studies have reported that luminance changes in the background delay and suppress responses to contrast<sup>28,29</sup>. Although these studies shed light on the response properties of uniform luminance-sensitive cells, we still largely lack understanding of the relevance of these cells in visual functions.

V1 cells are sensitive to transiently changing contrast that resembles natural stimulation<sup>30</sup>. Since responses to both diffuse light and uniform luminance contain transient components<sup>19,22</sup>, it is possible that V1 cells also respond to such briefly presented luminance stimuli that resemble the luminance variations occurring in natural



vision. To address the roles of uniform luminance-sensitive cells in processing transiently changing luminance, we investigated responses of cat V1 cells to large patches of uniform stimuli or grating stimuli that changed rapidly and consecutively in luminance and compared the speed preferences of luminance-contrast cells and contrast cells to the conventional drifting sinusoidal gratings. We show that the cells preferring decrements in luminance of uniform stimuli tend to prefer high speeds of motion. The results argue for a functional role for the luminance-sensitive cells in the detection of motion especially under dim light conditions.

## Results

We presented uniform stimuli (0% contrast) and spatial stimuli (static sinusoidal gratings of 100% contrast, Fig. 1a) of different luminances to cells in cat V1. When the stimulus size  $\leq$  RF, the contrast generated at the stimulus border by the difference between stimulus luminance and background luminance strongly impacted the neuronal responses. The effects were particularly strong for responses to uniform stimuli. Therefore, we used large circular stimuli with

diameters at least 3 times larger than the size of the classical receptive field (RF) of the cell<sup>17,19,26,27</sup>. The contrast effects on responses to the luminance of the interior of the stimulus patch were also removed by blurring the border with a smooth change in luminance from the stimulus level to the background (25  $\text{cd/m}^2$ ; Fig. 1a). Uniform stimuli included eleven luminance values from 0 to 50  $\text{cd/m}^2$  in steps of 5  $\text{cd/m}^2$  (5 of them decreasing and 5 increasing from the mean of 25  $\text{cd/m}^2$ , and the remaining one equal to the mean luminance). Gratings had a mean luminance equal to those of the eleven uniform stimuli (individually corresponding to 0–50  $\text{cd/m}^2$  in steps of 5  $\text{cd/m}^2$ ). The stimulus luminances were mostly within 1–1.5 log unit ranges that are typical of natural images<sup>31</sup>. Uniform stimuli were presented randomly one after another, each for 40 ms without blank intervals (the subspace reverse correlation method)<sup>34–37</sup>, and gratings were presented in the same way in a separate block (Fig. 1a). Thus, the luminance changes having different magnitudes in both presentations were random. The stimulus presentation simulated luminance changes carried by a uniform stimulus or a spatial contrast stimulus that often occur in natural vision. Note that the sole difference between the two kinds of stimuli was that the gratings had 100% contrast and the uniform stimuli had 0% contrast. The stimulus contrast was constant in a block of gratings presentations and therefore differed from our previous study<sup>21</sup> in which the stimulus contrast varied slowly and sinusoidally.

Luminance response functions (LRFs) were extracted from responses to different stimulus luminances at the time of the largest response variance when a cell showed the best tuning. Figs. 1b and 1c depict LRFs of a V1 cell to uniform stimuli and to grating stimuli. This cell was significantly tuned (see Data Analyses) to luminances of both kinds of stimuli. In a population of cells, 41% (109/269) showed this response behavior. Since the gratings contained 100% contrast, this group of cells was denoted as luminance-contrast cells. Many other cells (56%, 151/269) did not respond to uniform stimuli but only responded significantly to the luminances of the contrast gratings (i.e., contrast cells). An example of the latter cells is shown in Figs. 1e and 1f. The remaining cells (3%, 9/269) responded only to uniform luminance but not to gratings (i.e., luminance cells; not shown). Note that by distinguishing luminance-contrast cells and contrast cells in the current study we do not mean to classify V1 cells in the same manner as simple and complex cells and that within the confines of presenting large uniform and grating stimuli, V1 cells appear to be luminance-contrast cells or contrast cells. In fact, in the current experiment, responses to gratings were modulated by the luminances, but not by the contrasts, of the static gratings, because all gratings had the same 100% contrast. The variations in responses were due to luminance changes of the gratings. Responses to the luminance changes, however, were affected predominantly by the contrast of grating stimuli because, in general, these responses were stronger in magnitude than those to the luminance changes of uniform stimuli (Figs. 1b, 1c, 1e, 1f) and were monotonic increases (Figs. 1c, 1f), which is the typical response profile to stimulus contrast<sup>8</sup>. In our previous study<sup>21</sup>, the responses of cells to contrast stimuli were modulated by the sinusoidally changing contrast at a single border, and in the current study, the responses of cells to contrast gratings were evoked by luminance changes. Although these responses to the two types of contrast stimuli are somewhat different, the response properties of luminance-contrast cells and contrast cells in both studies are similar. Here we still use the terms of luminance-contrast cells and contrast cells to conveniently facilitate the succinct depiction of our current study and in relation to our previous work<sup>21</sup>.

These 269 cells were recorded from the region representing the central visual field across all cortical layers of V1. Their basic response properties, including RF position, size, and structure, were similar to those reported in our previous study<sup>21</sup>. To discriminate simple cells and complex cells, we analyzed the modulated responses of all cells to drifting gratings at 100% contrast. Crowder et al. (2007)

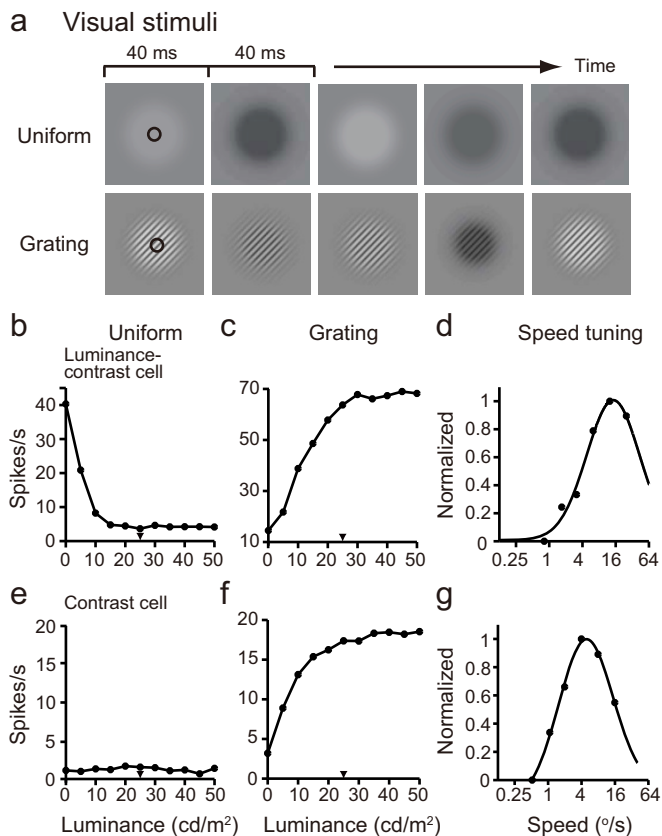


**Figure 1 | Visual stimuli and responses of V1 cells to luminance and motion speed.** (a) Luminance stimuli. Each stimulus was presented for 40 ms and all stimuli were presented successively and randomly without interval in a block. Uniform and grating stimuli were in separate blocks. Upper panels: uniform luminance stimuli (0% contrast); Lower panels: luminance expressed by grating stimuli (100% contrast). Dark circles indicate the receptive field of a cell. (b,c) Luminance response functions (LRFs) of a luminance-contrast cell to uniform and grating stimuli, respectively. (e,f) LRFs of a contrast cell. (d,g) The speed tuning curves of the two cells used as examples in (b,c) and (e,f). The X-axis is a logarithmic scale of motion speeds. The Y-axis is the normalized response by the maximal response. In (b), (c), (e), (f), the dots are raw data. In (d), (g), the dots are the normalized data after normalization by the maximal response and the lines are the fitted curves. Arrow heads in (b), (c), (e), (f) indicate the background luminance (25  $\text{cd/m}^2$ ).



have shown that  $F_1/F_0$  values of complex cells depend on the stimulus contrast, but those of simple cells do not, and concluded that only the cells with a modulation index ( $F_1/F_0$ ) > 1 in response to 100% contrast gratings can be regarded as real simple cells<sup>38</sup>. Based on this strict criterion, 15% of the cells (40/269) in our sample were simple cells and 85% (229/269) were complex cells ( $F_1/F_0 < 1$ ). The percentage of simple cells was reported as approximately 11% by Crowder et al.<sup>38</sup> and was 13% in our previous sample<sup>21</sup>.

We examined the relationships between contrast cells vs luminance-contrast cells and simple cells vs complex cells. Of the sampled cells, 17% (18/109) of luminance-contrast cells, 13% (20/151) of contrast cells, and 22% (2/9) of luminance cells were simple cells. We also analyzed the RF spatiotemporal structure of luminance-contrast cells and contrast cells by calculating the spatial and temporal overlap indices of ON and OFF subregions<sup>21</sup> measured with sparse stimuli presented by the reverse correlation method<sup>32,33</sup>. Overall, no clear differences were observed between luminance-contrast cells and contrast cells in relation to the classes of simple cells vs complex cells and to the spatiotemporal organization of their RF ON-OFF subregions. This result is consistent with our previous study<sup>21</sup> in which luminance-contrast cells and contrast cell were identified by slowly and sinusoidally changing luminance and contrast. Possibly the distinctions between luminance-contrast cells vs contrast cells and simple cells vs complex cells and the related RF ON-OFF structure largely lie in the large size of the stimuli we applied. With a large stimulus, a cell must integrate inputs from a region far beyond the classical RF. Responses to luminance decrements and increments in a large field are quite different from ON and OFF responses evoked by the sparse, small stimuli used to map a RF. Responses evoked by the large stimulus are also distinct from the modulated responses evoked by the drifting sinusoidal gratings used to measure  $F_1/F_0$  values. In the following sections, we therefore analyzed the response properties of luminance-contrast cells and contrast cells without regard to the simple and complex classes.

We compared the speed selectivity of the luminance-contrast cells with the contrast cells. The tuning curves of the V1 cells to motion speeds were measured for sinusoidal gratings drifting at different speeds along the preferred directions of motion for each cell. Note that the speed tunings we studied here were measured at the preferred spatial frequency of each V1 cell (see Methods). Fig. 1d plots the fitted speed tuning curve of a typical luminance-contrast cell with a preferred speed at 10.0 °/s, while Fig. 1g is for that of a typical contrast cell with a preferred speed at 4.25 °/s. This example of a luminance-contrast cell had a preferred motion speed higher than the example of the contrast cell. The averaged speed tuning curves from raw data of responses across 109 luminance-contrast cells and 151 contrast cells are shown in Fig. 2g. It is obvious that luminance-contrast cells and contrast cells differ in their ranges of preferred speeds. The speed tuning curves of individual cells were fitted by a log-Gaussian function [equation (2)] to obtain the preferred speed (defined as the peak of the fitted curves, e.g., Figs. 1d,1g) for the drifting gratings. The distributions of preferred speeds of the population of contrast cells and of the population of luminance-contrast cells are shown in Figs. 2h and 2i, respectively. The mean preferred speed of contrast cells was  $4.6 \pm 0.20$  °/s (mean  $\pm$  s.e.m;  $n = 151$ ; Fig. 2h) and that of luminance-contrast cells was  $8.6 \pm 0.24$  °/s ( $n = 109$ ; Fig. 2i). The difference was statistically significant (One-way ANOVA,  $P < 0.0001$ ), indicating that luminance-contrast cells prefer higher motion speeds than contrast cells at the population level.

The difference in speed tuning could be attributed either to the differences in responses of neurons to the spatial frequencies (SFs) or to the temporal frequencies (TFs) of drifting sinusoidal gratings. We further examined the SF and TF tunings of the luminance-contrast cells and the contrast cells. Figs. 2a and 2d show the averaged SF and TF curves of raw data for responses across the 109 luminance-contrast cells and the 151 contrast cells, respectively. It is noteworthy that

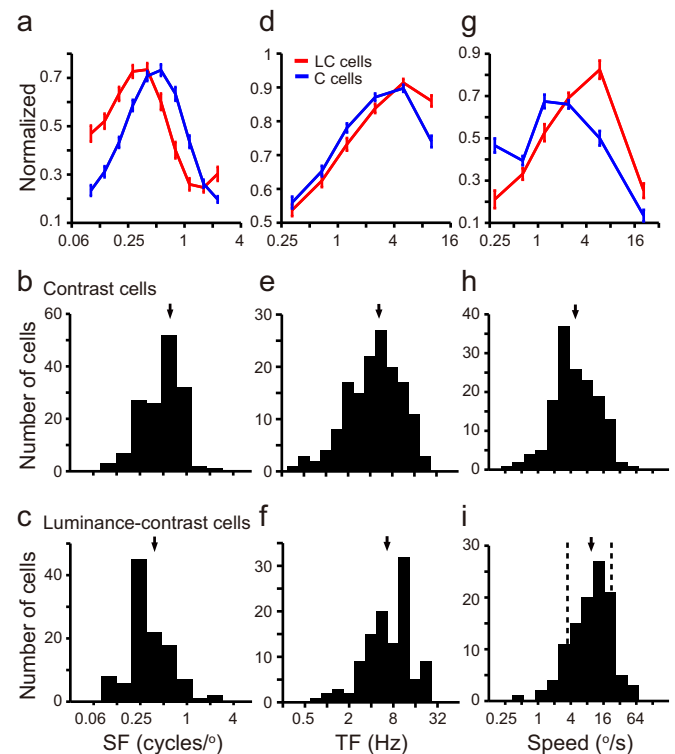


**Figure 2 | Luminance-contrast cells preferred lower SFs, higher TFs, and higher motion speeds than contrast cells.** (a,d,g) The averaged SF, TF, and speed response curves of raw data of 151 contrast cells and 109 luminance-contrast cells after normalization by the maximal response for each cell (e.g., Figs. 1d,1g). LC: luminance-contrast; C: contrast. The vertical lines show the s.e.m. (b,e,h) Distributions of preferred SFs, TFs, and motion speeds of 151 contrast cells. (c,f,i) Distributions of those of 109 luminance-contrast cells. The X-axis is a logarithmic scale of SFs, TFs, and motion speeds. Arrows indicate the mean values. In (i), the vertical dashed lines indicate  $\pm$  SD of preferred speeds for the data analysis of Fig. 5a.

the luminance-contrast cells show large differences in the SF tuning and small differences in TF tuning compared to the contrast cells. The SF and TF tuning curves of individual cells were fitted by a difference of Gaussian (DOG) functions [equation (1)] and a log-Gaussian function [equation (2)], respectively. Figs. 2b,2e and 2c,2f display the distributions of preferred SFs and TFs of contrast cells and luminance-contrast cells, respectively. The mean preferred SF of contrast cells was  $0.55 \pm 0.024$  cycles/° ( $n = 151$ ; Fig. 2b) and that of luminance-contrast cells was  $0.40 \pm 0.030$  cycles/° ( $n = 109$ ; Fig. 2c). This difference was significant (One-way ANOVA,  $P < 0.001$ ). These tuning curves to SFs were obtained using static sinusoidal gratings flashed consecutively, each for 40 ms (subspace reverse correlation method). The data confirm the preliminary result from a relatively small number of sample cells in our previous study in which SFs were tested using drifting gratings<sup>21</sup>. Thus, different tests show similar results, namely, that luminance-contrast cells prefer low SFs in comparison to contrast cells. The average of the preferred TFs of contrast cells was  $4.1 \pm 0.15$  cycles/s ( $n = 151$ ; Fig. 2e) and that of luminance-contrast cells was  $5.4 \pm 0.20$  cycles/s ( $n = 109$ ; Fig. 2f). Again this difference was significant (One-way ANOVA,  $P < 0.01$ ). Thus, both differences in SFs and TFs tuning possibly contribute to the difference of speed tunings between luminance-contrast cells and contrast cells.

One can ask whether luminance-contrast cells have response latencies that are shorter than those of contrast cells because they prefer faster drifting gratings. Therefore, we analyzed response latencies using the responses to the drifting gratings in the preferred

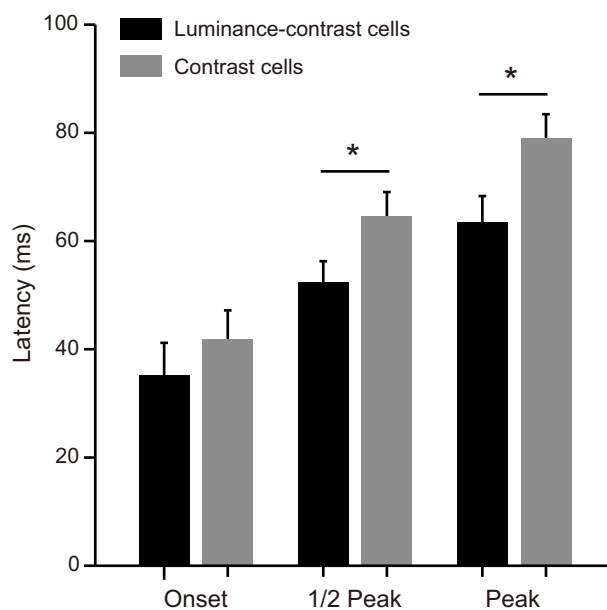


**Figure 3 | Response latencies of 109 luminance-contrast cells and 151 contrast cells to drifting sinusoidal gratings along the preferred directions of the cells.** The bars and vertical lines show the mean  $\pm$  s.e.m.; \* and the horizontal lines show the one-way ANOVA,  $P < 0.05$ . Onset: latency of the onset significant response; 1/2 peak: latency of half peak response; Peak: latency of the peak response.

direction of each cell rather than using the responses to the flashed stimuli. At the times when a cell showed the onset of the significant responses, the half peak magnitude, and the peak magnitude of responses were computed. The time of the onset significant response was defined as the first point of five consecutive data points (in a step of 1 ms) in which all five data points had to meet the criterion for the significant response, that is, the response magnitude beyond the mean  $\pm$  2 SDs of the baseline spikes. From Fig. 3, it can be seen that differences of response latencies between luminance-contrast cells and contrast cells gradually increased from the onset time ( $35 \pm 6.2$  ms,  $n = 109$  vs  $41.9 \pm 5.3$  ms,  $n = 151$ ), half peak time ( $52.3 \pm 3.9$  ms,  $n = 109$  vs  $65.7 \pm 4.4$  ms,  $n = 151$ ) to the peak time ( $62.3 \pm 3.6$  ms,  $n = 109$  vs  $79.0 \pm 4.5$  ms,  $n = 151$ ). The difference was significant for the response latencies at the half peak magnitude and at the peak magnitude (One-way ANOVA,  $P < 0.05$ ). These data suggest that responses of luminance-contrast cells to drifting gratings reach their peak magnitude more rapidly on average than do those of contrast cells.

Most luminance-sensitive cells respond to decrements in luminance<sup>20,21</sup>. In the current experiment, a cell might respond to luminance decrements (monotonically decreased LRF, e.g., Fig. 1b) or luminance increments (monotonically increased LRF) at the peak of its response variance curve, or to both at the peak and the sub-peak of the curve (e.g., Figs. 4a–c). In the sample of luminance-contrast cells, 50% (54/109) of cells had two peaks in response to both luminance decrements and increments (dark and light gray bars in Fig. 4d). Here, in order to quantitatively study the preference of a cell for luminance increments (lightening) and luminance decrements (darkening), its relative response strength to the increments and decrements was evaluated by an increment-decrement response index (IDRI). The responses of a cell to luminance increments and/or decrements were assessed with a stricter statistical criterion (see Data Analyses). A value 1 of IDRI indicates that a cell only responds significantly to luminance increments, 0 indicates no bias in response to either increments or decrements, and  $-1$  indicates that a cell responds only to decrements. The example cell shown in Figs. 4a–c had  $-0.20$  of IDRI, responding better to luminance decrements than

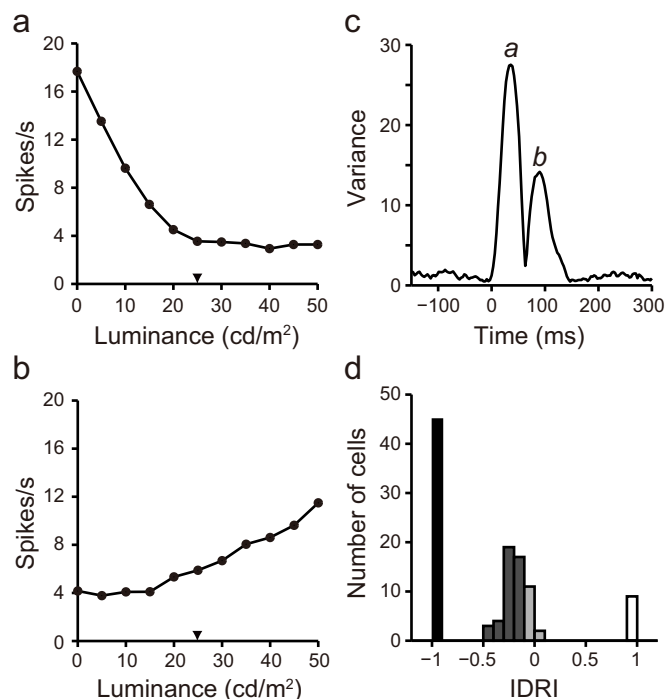


**Figure 4 | Uniform luminance-sensitive cells strongly preferred luminance decrements.** (a) Strong responses of a cell to luminance decrements at the response latency labeled with *a* in the variance curve of panel (c). (b) Weak responses of this cell to luminance increments at the response latency labeled with *b* in the variance curve of panel (c). Dots: raw data. (c) Variance curve of responses of this cell to uniform luminance stimuli. Curves in panels (a) and (b) are responses of this cell to luminance decrements and luminance increments at the times of the response variance curve indicated by *a* and *b* in panel (c), respectively. The cell had the first peak at 36 ms (*a*) and the secondary peak at 88 ms (*b*). Among the luminance-contrast cells having two significant response peaks (dark and light gray bars in Fig. 4d), the average first peak time was  $53.9 \pm 2.8$  ms (mean  $\pm$  s.e.m.,  $n = 54$ ) and the second peak time was  $84.7 \pm 4.7$  ms. The mean difference between the two peak times was  $30.8 \pm 1.9$  ms. (d) Distribution of increment-decrement response indices (IDRI; X-axis) of 109 luminance-contrast cells. Dark bar: the cells responded only to luminance decrements, IDRI =  $-1$ ; Dark gray bars: the cells responded to luminance decrements more strongly than to increments,  $-1 < \text{IDRI} < -0.1$ ; Light gray bars,  $-0.1 \leq \text{IDRI} \leq 0.1$ : the cells responded equally to luminance decrements and increments; Light bar: the cells responded only to luminance increments, IDRI =  $1$ . Arrow heads in (a), (b) indicate the background luminance ( $25 \text{ cd/m}^2$ ).

to increments. The mean IDRI of all luminance-contrast cells was  $-0.40$ , indicating a strong response bias to luminance decrements at the population level. Among the cells, 42% (46/109) responded only to decrements (IDRI =  $-1$ , dark bar in Fig. 4d), 34% (37/109) had a larger response magnitude to decrements than to increments ( $-1 < \text{IDRI} < -0.1$ , dark gray bars in Fig. 4d), 16% (17/109) had approximately equal responses to decrements and increments ( $-0.1 \leq \text{IDRI} \leq 0.1$ , light gray bars in Fig. 4d), and the remaining 8% (9/109) responded only to increments (IDRI =  $1$ , light bars in Fig. 4d). Therefore, there are many more luminance-contrast cells responding strongly to luminance decrements than to increments.

Since the above results show that luminance-contrast cells prefer higher speeds and most of them respond better to luminance decrements, do the cells selective for high speeds, for example, those on the right side in Fig. 2i, really tend to prefer luminance decrements? To address this question, we analyzed the relationship between IDRIs and preferred motion speeds of the luminance-contrast cells. The scatter plot between the IDRIs and the preferred speeds for these





cells, however, did not show a clear correlation because the distribution of IDRIs was widely separated, that is, as shown in Fig. 4d, forming three clusters. Therefore, we explored the relationship in the other ways by dividing these luminance-contrast cells into different groups based on either their preferred speeds or their IDRIs. Using their preferred speeds, 109 luminance-contrast cells were divided into three groups: one group of cells ( $n = 14$ ) had a preferred speed  $< (\text{mean} - \text{SD})$  shown by the left dashed line in Fig. 2i (slow speed); the other group ( $n = 15$ ) had a preferred speed  $> (\text{mean} + \text{SD})$  shown by the right dashed line in Fig. 2i (fast speed); and the third group ( $n = 80$ ) had a preferred speed between  $(\text{mean} - \text{SD})$  and  $(\text{mean} + \text{SD})$  shown by the intermediate region between the two dashed lines in Fig. 2i (medium speed). Then, the mean IDRIs of the three groups of cells were calculated. Overall, all three groups had negative IDRIs, indicating that in each group most cells preferred luminance decrements. The mean IDRIs of the slow, medium, and fast speed groups of cells were  $-0.21 \pm 0.23$  ( $n = 14$ ),  $-0.41 \pm 0.05$  ( $n = 80$ ), and  $-0.54 \pm 0.19$  ( $n = 15$ ). From Fig. 5a, it can be seen that the mean IDRI tended to be more negative when the preferred speeds increased. This decrease in the IDRIs with the increase in the preferred speeds was statistically significant (One-way ANOVA,  $P < 0.05$ ). On the other hand, the luminance-contrast cells were divided into three groups according to their IDRIs: one group of cells only responsive to luminance decrements ( $\text{IDRI} = -1$ ; dark bars of Figs. 4d,5b) on average had a preferred speed of  $11.3 \pm 2.14$  °/s ( $n = 46$ ); the other group responsive to both decrements and increments ( $-0.5 \leq \text{IDRI} \leq 0.1$ ; gray bars of Figs. 4d,5b) had a preferred speed of  $8.3 \pm 2.36$  °/s ( $n = 54$ ); and the third group responsive only to increments ( $\text{IDRI} = 1$ ; light bars of Figs. 4d,5b) had a preferred speed of  $5.9 \pm 2.14$  °/s ( $n = 9$ ). The mean preferred speeds of the three groups of cells significantly decreased when their IDRIs increased (Fig. 5b; One-way ANOVA,  $P < 0.05$ ). Thus, these results analyzed from the standpoints of both preferred speed and IDRI support the view that luminance-contrast cells preferring high speeds are more likely to respond to luminance decrements.

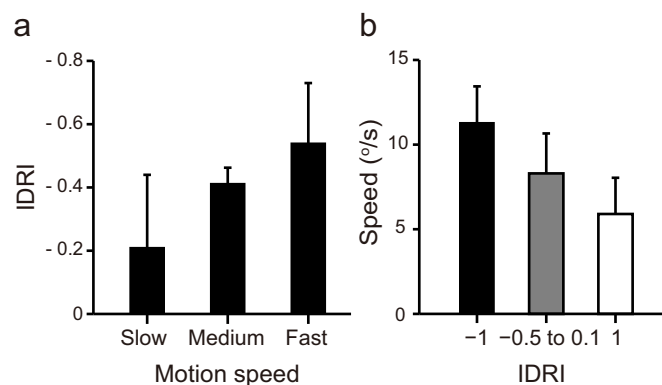


**Figure 5 | Relationship between the preferences of luminance-contrast cells for motion speeds and for luminance decrements vs increments.** (a) Mean IDRIs of three groups of luminance-contrast cells having slow, medium, and fast speeds. The 109 cells were divided by the  $(\text{mean} - \text{SD})$  and  $(\text{mean} + \text{SD})$  of the preferred speeds of all luminance-contrast cells shown in Fig. 2i into the groups with slow ( $n = 14$ ), medium ( $n = 80$ ), and fast speeds ( $n = 15$ ). For details, see the main text. (b) Mean speeds of three groups of luminance-contrast cells responsive only to luminance decrements ( $\text{IDRI} = -1$ , dark bar;  $n = 46$ ), to both luminance decrements and increments ( $-0.5 < \text{IDRI} \leq 0.1$ , gray bar;  $n = 54$ ), and only to luminance increments ( $\text{IDRI} = 1$ , light bar;  $n = 9$ ). For IDRI distribution of these luminance-contrast cells, see Fig. 4d. For details, see the main text. In (a), (b), the bars and vertical lines: mean  $\pm$  s.e.m.

## Discussion

Our main finding is that in cat V1 the cells responsive to uniform luminance prefer more rapidly moving stimuli than the cells responsive only to the luminances expressed by contrast stimuli. Most uniform luminance-sensitive cells also strongly prefer luminance decrements over luminance increments. These cells also respond to contrast, orientation, and SF of visual stimuli<sup>21</sup>. Based on these response properties, we speculate that luminance-sensitive cells in cat V1 play roles in motion processing under conditions of dim illumination.

It is well known that in the cat's retinogeniculate pathway, Y cells tend to prefer lower SFs and higher speeds much as magnocellular cells and X cells prefer higher SFs and lower speeds much as parvocellular cells in primates<sup>39–44</sup>. Here we show that luminance-contrast cells prefer low SFs, high TFs, and high speeds, like Y cells, whereas contrast cells prefer high SFs, low TFs, and low speeds, like X cells. The correlated relationships between the retinogeniculate cells and the cortical cells in these response properties suggest that the input of the retinogeniculate Y pathway contributes to the responses of luminance-contrast cells to low SFs, high TFs and high speeds, and that of the X pathway contributes to the responses of contrast cells. The results of SFs, TFs, and motion speeds further support the roles of Y pathway in the generation of responses of luminance-contrast cells to uniform luminance in V1 discussed in our previous study<sup>21</sup>.

Uniform stimuli are the extreme of low SFs. Thus, responses of luminance-contrast cells to uniform luminance can be attributed to their tuning preference for the lower SFs. Moreover, their preference for high speeds can be accounted for by their tuning preferences for low SFs and high TFs. The response tunings of most V1 cells to SFs and TFs are separable. The separability of SF and TF tunings leads to the view that the SF and TF tunings are independent, that is, the SF that evokes the best response is the same across TFs, and *vice versa*. Thus, the preferred speed of V1 cells decreases as a function of SF and increases as a function of TF<sup>45</sup>. The model of speed tuning in relation with SFs and TFs predicts that the cells preferring lower SFs respond best to higher speeds and the cells preferring higher TFs also respond best to higher speeds. Therefore, the preferences of luminance-contrast cells for lower SFs and higher TFs determine their preference for higher speeds and the preferences of contrast cells for higher SF and lower TF determine their preference for lower speeds. It is possible that the tuning preference of luminance-contrast cells for high speeds is built upon the inputs of the subcortical Y pathway carrying the low SF and high TF information and is further strengthened by the intracortical circuits that emphasizes the processing of the motion and luminance information.

Luminance and contrast information are largely processed independently in the early visual pathway from retina to geniculate to V1<sup>12,21,31,46,47</sup>. The coding strategy endows the visual system with the advantages of detecting contrast across variations in luminance and detecting luminance across variations in contrast. Thus, the finding that most luminance-sensitive cells prefer fast motion and luminance decrements is of special behavioral and ecological significance because these cells signal fast moving stimuli even when light illumination decreases. This would aid perception and help an animal navigating through a low visibility environment, such as dark night and fog. This would also be particularly useful to a nocturnal species such as a cat which hunts at night but is small and therefore vulnerable to predators. Each species adapts to its own natural environment. Cats have excellent night vision and are much more sensitive to the low light level than primates<sup>48</sup>. This is partly because cat eyes have a *tapetum lucidum* which increases the sensitivity to dim light<sup>49</sup>. Thus, it is not unexpected that we found cells in cat V1 signaling information about stimuli moving at a high speed in conditions that would be deemed poor visibility for primates.

Using artificial stimuli with carefully designed parameters is the most effective method for in advancing our understanding of visual



functions<sup>1–3,50</sup>. The transient luminance changes (with a timescale of 40 ms) carried by uniform stimuli and spatial stimuli such as the ones we used are similar to what occurs in natural vision<sup>47,51,52</sup>. The transient stimuli were well parameterized in terms of luminance, which ranged from 0 to 50 cd/m<sup>2</sup> in steps of 5 cd/m<sup>2</sup>, and of contrast, which was maintained constant at 0% or 100%. The stimuli are somewhat simpler than natural stimuli<sup>2,50,53–55</sup>, but also contain the richness of natural stimuli in the dimension of luminance change because the random presentation of stimulus luminances simulates natural luminance changes<sup>47,51,52</sup>. The dynamic luminance stimuli combined with the traditional drifting spatial gratings captures response behaviors of V1 luminance-contrast cells to transiently changing luminances, revealing the functional roles of these cells in visual motion.

## Methods

**Physiological preparations.** All animal care and experimental procedures conformed to the guidelines of the National Institutes of Health (USA) and were approved by Institutional Animal Care and Usage Committee of The Institute of Biophysics, Chinese Academy of Sciences. Twenty-four normal adult cats (2–3 kg) were prepared for single-unit recording using procedures described in a previous study<sup>21</sup>. Animal anesthesia was induced by ketamine (20–30 mg/kg, i.m.) after injection of dexamethasone and atropine (i.m.). During recording, anesthesia and paralysis were maintained with an infusion of sufentanil (0.15–0.22 µg/kg/hr, i.v.), propofol (1.8–2.2 mg/kg/hr, i.v.), and gallamine triethiodide (10 mg/kg/hr, i.v.) in a Ringers solution containing 5% glucose. The corneas were protected with contact lenses that had sufficient power with 3 mm artificial pupils to focus the eyes on a CRT monitor at a distance of 57 cm. A glass-coated tungsten electrode (1–3 MΩ) and a TDT amplifier and data acquisition system (TDT, Inc, Florida) at a sample rate of 12 kHz were used to record extracellular action potentials from neurons in V1 (centered at Horsley-Clarke coordinates P 2.5 mm and L 2.5 mm) where their RFs represented the central visual field. Individual units were further identified off-line with a TDT OpenSorter. The time delay for the recording system from stimulus generation to data acquisition was calibrated.

**Visual stimuli.** Stimuli were displayed on a CRT monitor (Iiyama HM204DT A, 800 × 600 pixel resolution, 100 Hz refresh rate) that subtended 40 × 30° in visual angle in a dark room (0.1 cd/m<sup>2</sup> measured using ColorCAL colorimeter [CRS, Ltd]). The display was calibrated to remove luminance nonlinearities and obtain a precise match between the requested and actual luminances. The animal and the space between the animal and the monitor were covered or surrounded with black boards to allow the eyes of the animal to face only the display in order to avoid scatter effects from other light sources and reflections. The size and location of the RF for the dominant eye of cells being recording were explored with stimuli controlled by a computer mouse, and the other eye was covered. After the preliminary tests, the preferred orientation (0°–165° in 15° steps) and spatial frequency (SF, 0.1–2.3 cycles/°) were measured quantitatively using the subspace reverse correlation technique with sinusoidal gratings<sup>34–37</sup>, and the classical RFs were measured quantitatively using the reverse correlation technique with static white and dark short bars (1.5° × 0.5°)<sup>32,33</sup>. Preference for motion direction and temporal frequency (TF) were measured with 100% sinusoidal gratings having the preferred SF and drifting along the preferred direction. For a cell, the exact sampled data points of TF (0.125–10 Hz) were dependent on the preferred TF of the cell.

Uniform and spatial stimuli were applied to study responses of a cell to luminance. Both stimuli had the same size. The width of blurred regions equaled to those of non-blurred regions of the stimuli (Fig. 1a). For the luminance expressed by a spatial contrast stimulus, all gratings had 100% contrast (defined by Michelson contrast for a spatially periodic pattern), the preferred orientation, and preferred SF of the cell. Each grating stimulus contained 8 spatial phases (0–7 π/4 in a step of π/4). Each stimulus was presented for 40 ms and repeated at least 800 times. For other stimulus parameters, see the main text.

**Data analyses.** Responses to a given stimulus luminance were sorted using the reverse correlation method from the spike train recorded from a cell to a stimulation sequence in order to obtain the average firing rate<sup>34–37</sup>. In the reverse correlation algorithm, an array of counters corresponding to each of the stimuli was reset to zero. To relate a stimulus to the spikes evoked by it in a spike train recorded,  $\tau$  denoted the time delay of the spikes after stimulus onset. For each spike, we went back  $\tau$  ms in time to look for the stimulus corresponding to the spike at that moment in the stimulus sequence. The counter corresponding to that stimulus had one added to it. For grating stimuli, responses to gratings having the same luminance but at 8 spatial phases were sorted to the same counter. Responses to a stimulus at a delay time of  $\tau$  were counted across the spike train. The time course of responses was generated by shifting  $\tau$  from –150 ms to 300 ms in 1 ms steps. The variance curve of responses of a cell to different uniform stimuli or grating stimuli was calculated with a 1 ms resolution (e.g., Fig. 4c). At the true response (optimal) latency, a cell responded best to the preferred stimulus and poorly to the non-preferred stimulus, therefore it had the maximal variance of responses to different stimuli and had the best tuning curve. To

take an objective criterion for data selection, we estimated the noise level of responses by calculating the variance of spikes to all stimuli,  $\tau$  from –150 to 0 ms, before stimulus onset. The mean and SD of these variances were obtained. The mean + 4 SDs of variances of the noise spikes from –150 to 0 ms (noise level) were taken as the criterion<sup>36,37</sup>. We accepted the data in which the maximal value of response variances to different luminances after stimulus onset exceeded this criterion of noise level. Luminance response functions (LRFs) were extracted from responses to different luminance stimuli at the time of the peak or at the secondary peak variance (e.g., Figs. 4a–c).

The SF tuning curve was fitted by difference of Gaussian (DOG) functions:

$$R(sf) = R_0 + P_e e^{-((sf - \mu_e)/2\sigma_e)^2} - P_i e^{-((sf - \mu_i)/2\sigma_i)^2} \quad (1)$$

and  $R_0$ ,  $P_e$ ,  $P_i$ ,  $\mu_e$ ,  $\mu_i$ ,  $\sigma_e$  and  $\sigma_i$  were optimized to provide the least squared error fit to the data. The preferred SF is the peak of SF curve<sup>36</sup>.

The motion speeds were calculated by  $V$  (°/s) = TF (cycles/s) / SF (cycles/°). The speed (s) tuning curve was fitted by a log-Gaussian function:

$$R(s) = R_0 + A \times \exp \left[ -\frac{1}{2 \times \sigma^2} \left( \log \frac{s + s_0}{s_p + s_0} \right)^2 \right] \quad (2)$$

and  $R_0$ ,  $A$ ,  $s_0$ ,  $s_p$ , and  $\sigma$  are free parameters.  $s_p$  is the preferred speed, and  $\sigma$  is the width of the curve (in log speed)<sup>37,58</sup>. The TF tuning curve was also fitted by the log-Gaussian function.

To compare responses of a cell to luminance increments and decrements, a increment-decrement response index (IDRI) is defined as:

$$IDRI = \frac{R_{Increment} - R_{Decrement}}{R_{Increment} + R_{Decrement}} \quad (3)$$

where  $R_{Increment}$  is response magnitude to luminance increasing from 25 cd/m<sup>2</sup> of the average luminance to 50 cd/m<sup>2</sup> and  $R_{Decrement}$  is response magnitude to luminance decreasing from 25 cd/m<sup>2</sup> of the average luminance to 0 cd/m<sup>2</sup>, respectively. The responses of a cell to luminance decrements and increments were evaluated with a stricter statistical criterion. The evaluation was based only on responses to three decrement stimuli of 0, 5, and 10 cd/m<sup>2</sup> and on those to three increment stimuli of 40, 45, and 50 cd/m<sup>2</sup>. Response variances to the two groups of stimuli were calculated from 0 ms to 300 ms in 1 ms steps, respectively. Only the responses that met the criterion for a significant response, that is, a variance of responses to the group of three stimuli was beyond the mean ± 4 SDs of the variances of the noise spikes from –150 to 0 ms, were included in the IDRI analysis. Then, we determined the times at which the largest response variance occurred when the cell showed the best tuning to luminance decrements of the three stimuli or to luminance increments of the three stimuli. Next, the maximal responses ( $R_{Increment}$  and/or  $R_{Decrement}$ ) were extracted from the monotonic response curves to the three increment stimuli and/or to the three decrement stimuli at the times of the largest variance, respectively. If the response of a cell to increment or decrement stimuli did not meet the criterion for a significant response, its  $R_{Increment}$  or  $R_{Decrement}$  was zero.

- Rust, N. C. & Movshon, J. A. In praise of artifice. *Nat Neurosci* **8**, 1647–1650 (2005).
- Felsen, G. & Dan, Y. A natural approach to studying vision. *Nat Neurosci* **8**, 1643–1646 (2005).
- Sharpee, T. O. Computational identification of receptive fields. *Annu Rev Neurosci* **36**, 103–120 (2013).
- Hubel, D. H. & Wiesel, T. N. Receptive Fields of Single Neurons in the Cats Striate Cortex. *J Physiol* **148**, 574–591 (1959).
- Hubel, D. H. & Wiesel, T. N. Receptive fields, binocular interaction and functional architecture in the cat's visual cortex. *J Physiol* **160**, 106–154 (1962).
- Movshon, J. A., Thompson, I. D. & Tolhurst, D. J. Spatial and temporal contrast sensitivity of neurones in areas 17 and 18 of the cat's visual cortex. *J Physiol* **283**, 101–120 (1978).
- Dean, A. The relationship between response amplitude and contrast for cat striate cortical neurones. *The Journal of Physiology* **318**, 413–427 (1981).
- Albrecht, D. G. & Hamilton, D. B. Striate cortex of monkey and cat: contrast response function. *J Neurophysiol* **48**, 217–237 (1982).
- Ohzawa, I., Sclar, G. & Freeman, R. D. Contrast Gain-Control in the Cat Visual-Cortex. *Nature* **298**, 266–268 (1982).
- Sclar, G., Lennie, P. & DePriest, D. D. Contrast adaptation in striate cortex of macaque. *Vision Res* **29**, 747–755 (1989).
- Bonds, A. B. Temporal dynamics of contrast gain in single cells of the cat striate cortex. *Vis Neurosci* **6**, 239–255 (1991).
- Lam, D. M.-K. & Shapley, R. *Contrast sensitivity*. Vol. 5, (The MIT Press, 1993).
- Allison, J. D., Casagrande, V. A., DeBruyn, E. J. & Bonds, A. B. Contrast adaptation in striate cortical neurons of the nocturnal primate bushy baby (*Galago crassicaudatus*). *Vis Neurosci* **10**, 1129–1139 (1993).
- Mechler, F., Victor, J. D., Purpura, K. P. & Shapley, R. Robust temporal coding of contrast by V1 neurons for transient but not for steady-state stimuli. *J Neurosci* **18**, 6583–6598 (1998).
- Albrecht, D. G., Geisler, W. S., Frazor, R. A. & Crane, A. M. Visual cortex neurons of monkeys and cats: temporal dynamics of the contrast response function. *J Neurophysiol* **88**, 888–913 (2002).



16. Crowder, N. A., Hietanen, M. A., Price, N. S. C., Clifford, C. W. G. & Ibbotson, M. R. Dynamic contrast change produces rapid gain control in visual cortex. *J Physiol* **586**, 4107–4119 (2008).
17. Rossi, A. F., Rittenhouse, C. D. & Paradiso, M. A. The representation of brightness in primary visual cortex. *Science* **273**, 1104–1107 (1996).
18. MacEvoy, S. P., Kim, W. & Paradiso, M. A. Integration of surface information in primary visual cortex. *Nat Neurosci* **1**, 616–620 (1998).
19. Kinoshita, M. & Komatsu, H. Neural representation of the luminance and brightness of a uniform surface in the macaque primary visual cortex. *J Neurophysiol* **86**, 2559–2570 (2001).
20. Peng, X. M. & Van Essen, D. C. Peaked encoding of relative luminance in macaque areas V1 and V2. *J Neurophysiol* **93**, 1620–1632 (2005).
21. Dai, J. & Wang, Y. Representation of surface luminance and contrast in primary visual cortex. *Cereb Cortex* **22**, 776–787 (2012).
22. Bartlett, J. R. & Doty Sr, R. W. Response of units in striate cortex of squirrel monkeys to visual and electrical stimuli. *J Neurophysiol* **37**, 621–641 (1974).
23. Kayama, Y., Riso, R. R., Bartlett, J. R. & Doty, R. W. Luxotonic responses of units in macaque striate cortex. *J Neurophysiol* **42**, 1495–1517 (1979).
24. DeYoe, E. A. & Bartlett, J. R. Rarity of fluxotonic responses in cortical visual areas of the cat. *Exp Brain Res* **39**, 125–132 (1980).
25. Maguire, W. M. & Baizer, J. S. Luminance coding of briefly presented stimuli in area 17 of the rhesus monkey. *J Neurophysiol* **47**, 128–137 (1982).
26. Roe, A. W., Lu, H. D. & Hung, C. P. Cortical processing of a brightness illusion. *Proc Natl Acad Sci U S A* **102**, 3869–3874 (2005).
27. Hung, C. P., Ramsden, B. M. & Roe, A. W. A functional circuitry for edge-induced brightness perception. *Nat Neurosci* **10**, 1185–1190 (2007).
28. Huang, X. & Paradiso, M. A. Background changes delay information represented in macaque V1 neurons. *J Neurophysiol* **94**, 4314–4330 (2005).
29. Tucker, T. R. & Fitzpatrick, D. Luminance-evoked inhibition in primary visual cortex: a transient veto of simultaneous and ongoing response. *J Neurosci* **26**, 13537–13547 (2006).
30. Hu, M., Wang, Y. & Wang, Y. Rapid dynamics of contrast responses in the cat primary visual cortex. *PLoS One* **6**, e25410 (2011).
31. Geisler, W. S., Albrecht, D. G. & Crane, A. M. Responses of neurons in primary visual cortex to transient changes in local contrast and luminance. *J Neurosci* **27**, 5063–5067 (2007).
32. Jones, J. P. & Palmer, L. A. The two-dimensional spatial structure of simple receptive fields in cat striate cortex. *J Neurophysiol* **58**, 1187–1211 (1987).
33. DeAngelis, G. C., Ohzawa, I. & Freeman, R. D. Spatiotemporal organization of simple-cell receptive fields in the cat's striate cortex. I. General characteristics and postnatal development. *J Neurophysiol* **69**, 1091–1117 (1993).
34. Ringach, D. L., Hawken, M. J. & Shapley, R. Dynamics of orientation tuning in macaque primary visual cortex. *Nature* **387**, 281–284 (1997).
35. Reid, R. C., Victor, J. D. & Shapley, R. M. The use of m-sequences in the analysis of visual neurons: linear receptive field properties. *Vis Neurosci* **14**, 1015–1027 (1997).
36. Bredfeldt, C. E. & Ringach, D. L. Dynamics of spatial frequency tuning in macaque V1. *J Neurosci* **22**, 1976–1984 (2002).
37. Nishimoto, S., Arai, M. & Ohzawa, I. Accuracy of subspace mapping of spatiotemporal frequency domain visual receptive fields. *J Neurophysiol* **93**, 3524–3536 (2005).
38. Crowder, N. A., Van Kleef, J., Dreher, B. & Ibbotson, M. R. Complex cells increase their phase sensitivity at low contrasts and following adaptation. *J Neurophysiol* **98**, 1155–1166 (2007).
39. Victor, J. D. & Shapley, R. M. Receptive field mechanisms of cat X and Y retinal ganglion cells. *J Gen Physiol* **74**, 275–298 (1979).
40. Sherman, S. M. & Spear, P. D. Organization of visual pathways in normal and visually deprived cats. *Physiol Rev* **62**, 738–855 (1982).
41. Shapley, R. & Perry, V. H. Cat and Monkey Retinal Ganglion-Cells and Their Visual Functional Roles. *Trends in Neurosciences* **9**, 229–235 (1986).
42. Burke, W., Dreher, B. & Wang, C. Selective block of conduction in Y optic nerve fibres: significance for the concept of parallel processing. *Eur J Neurosci* **10**, 8–19 (1998).
43. Troy, J. B. & Shou, T. The receptive fields of cat retinal ganglion cells in physiological and pathological states: where we are after half a century of research. *Prog Retin Eye Res* **21**, 263–302 (2002).
44. Nassi, J. J. & Callaway, E. M. Parallel processing strategies of the primate visual system. *Nat Rev Neurosci* **10**, 360–372 (2009).
45. Priebe, N. J., Lisberger, S. G. & Movshon, J. A. Tuning for spatiotemporal frequency and speed in directionally selective neurons of macaque striate cortex. *J Neurosci* **26**, 2941–2950 (2006).
46. Shapley, R. & Enroth-Cugell, C. *Visual adaptation and retinal gain controls*. Vol. 3, (Pergamon Press, 1984).
47. Mante, V., Frazor, R. A., Bonin, V., Geisler, W. S. & Carandini, M. Independence of luminance and contrast in natural scenes and in the early visual system. *Nat Neurosci* **8**, 1690–1697 (2005).
48. Case, L. P. *The cat: its behavior, nutrition & health*. (Iowa State Press, 2003).
49. Ollivier, F. J. *et al.* Comparative morphology of the tapetum lucidum (among selected species). *Vet Ophthalmol* **7**, 11–22 (2004).
50. David, S. V., Vinje, W. E. & Gallant, J. L. Natural stimulus statistics alter the receptive field structure of v1 neurons. *J Neurosci* **24**, 6991–7006 (2004).
51. Dong, D. W. & Atick, J. J. Statistics of Natural Time-Varying Images. *Network-Comp Neural* **6**, 345–358 (1995).
52. Lesica, N. A. *et al.* Dynamic encoding of natural luminance sequences by LGN bursts. *PLoS Biol* **4**, e209 (2006).
53. van Hateren, J. H. & van der Schaaf, A. Independent component filters of natural images compared with simple cells in primary visual cortex. *Proc Biol Sci* **265**, 359–366 (1998).
54. Sharpee, T., Rust, N. C. & Bialek, W. Analyzing neural responses to natural signals: maximally informative dimensions. *Neural Comput* **16**, 223–250 (2004).
55. Rapela, J., Mendel, J. M. & Grzywacz, N. M. Estimating nonlinear receptive fields from natural images. *J Vis* **6**, 441–474 (2006).
56. Sceniak, M. P., Hawken, M. J. & Shapley, R. Contrast-dependent changes in spatial frequency tuning of macaque V1 neurons: Effects of a changing receptive field size. *J Neurophysiol* **88**, 1363–1373 (2002).
57. Nover, H., Anderson, C. H. & DeAngelis, G. C. A logarithmic, scale-invariant representation of speed in macaque middle temporal area accounts for speed discrimination performance. *J Neurosci* **25**, 10049–10060 (2005).
58. Gao, E., DeAngelis, G. C. & Burkhalter, A. Parallel input channels to mouse primary visual cortex. *J Neurosci* **30**, 5912–5926 (2010).

## Acknowledgments

We thank Ray Guillery and Vivien Casagrande for their comments and improvements to the manuscript and Zhen Jiang for his assistance in the study. This study was supported by grants to YW from the National Natural Science Foundation of China (30570587, 30623004, 30870831), by National High-Tech Research & Development Program (2007AA02Z313 of 863 Program) of Ministry of Science and Technology, and by the Knowledge Innovation Program from Chinese Academy of Sciences (KSCX1-YW-R-32).

## Author contributions

Y.W. conceived the study, Y.W. and R.L. designed the experiment, R.L. performed the experiment, R.L. and Y.W. analyzed data, Y.W. and R.L. interpreted the results, Y.W. and R.L. wrote the manuscript.

## Additional information

**Competing financial interests:** The authors declare no competing financial interests.

**How to cite this article:** Li, R. & Wang, Y. Neural Mechanism for Sensing Fast Motion in Dim Light. *Sci. Rep.* **3**, 3159; DOI:10.1038/srep03159 (2013).



This work is licensed under a Creative Commons Attribution-NonCommercial-ShareAlike 3.0 Unported license. To view a copy of this license, visit <http://creativecommons.org/licenses/by-nc-sa/3.0>